Generalizable and Animatable Gaussian Head Avatar

Xuangeng Chu
The University of Tokyo
xuangeng.chu@mi.t.u-tokyo.ac.jp

Tatsuya Harada
The University of Tokyo
RIKEN AIP
harada@mi.t.u-tokyo.ac.jp

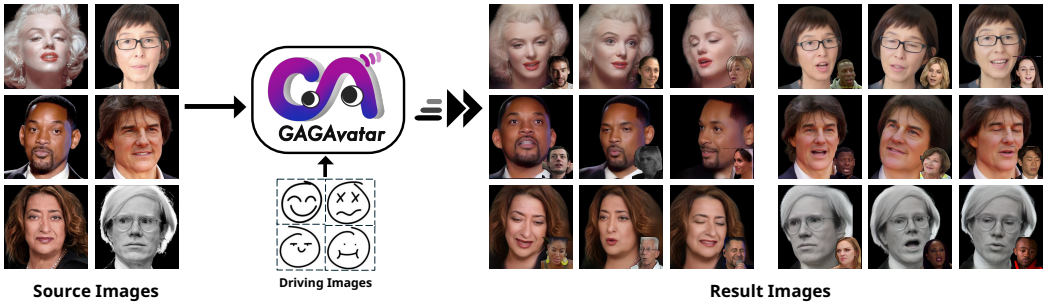

Figure 1: Our method can reconstruct animatable avatars from a single image, offering strong generalization and controllability with real-time reenactment speeds.

Abstract

In this paper, we propose **G**eneralizable and **A**nimatable **G**aussian head **A**vatar (GAGAvatar) for one-shot animatable head avatar reconstruction. Existing methods rely on neural radiance fields, leading to heavy rendering consumption and low reenactment speeds. To address these limitations, we generate the parameters of 3D Gaussians from a single image in a single forward pass. The key innovation of our work is the proposed dual-lifting method, which produces high-fidelity 3D Gaussians that capture identity and facial details. Additionally, we leverage global image features and the 3D morphable model to construct 3D Gaussians for controlling expressions. After training, our model can reconstruct unseen identities without specific optimizations and perform reenactment rendering at real-time speeds. Experiments show that our method exhibits superior performance compared to previous methods in terms of reconstruction quality and expression accuracy. We believe our method can establish new benchmarks for future research and advance applications of digital avatars. Code and demos are available at https://github.com/xg-chu/GAGAvatar.

1 Introduction

One-shot head avatar reconstruction has garnered significant attention in computer vision and graphics recently due to its great potential in applications such as virtual reality and online meetings. The typical problem involves faithfully recreating the source head from one image while precisely controlling expressions and poses. In recent years, many exploratory methods have achieved this goal using 2D generative models and 3D synthesizers.

Some early 2D-based methods [Yin et al., 2022, Ren et al., 2021] typically combine estimated deformation fields with generative networks to drive images. However, due to the lack of necessary 3D constraints and modeling, these methods struggle to maintain multi-view consistency of expressions and identities when head poses change significantly. Recently, Neural Radiance Fields (NeRF) [Mildenhall et al., 2020] have shown impressive results in head avatar synthesis, providing

38th Conference on Neural Information Processing Systems (NeurIPS 2024).

https://doi.org/10.52202/079017-1838

solutions using 3D synthesizers to achieve realistic details such as accessories and hair. However, some NeRF-based methods [Ma et al., 2023] require identity-specific training and optimization, and some methods [Li et al., 2023a, Chu et al., 2024, Deng et al., 2024a] can't render in real-time during inference, limiting their application in certain scenarios. With the emergence of 3D Gaussian splatting [Kerbl et al., 2023], some methods [Xu et al., 2024] have achieved real-time rendering. However, these methods still require specific training for each identity and fail to generalize to unseen identities, leaving the modeling of generalizable 3D Gaussian-based head models unexplored.

To address these limitations, we introduce a novel 3D Gaussian-based framework for one-shot head avatar reconstruction. Given a single image, our framework reconstructs an animatable 3D Gaussian-based head avatar, achieving real-time expression control and rendering. Some examples are shown in Fig. 1. The core challenge lies in faithfully reconstructing 3D Gaussians from a single image, as a 3D Gaussian typically requires multi-view input and millions of Gaussian points for detailed reconstruction. To address this, we propose a novel dual-lifting method that reconstructs the 3D Gaussians from one image. Specifically, instead of directly estimating Gaussian points from the image, we predict the lifting distances of each pixel relative to the image plane, and then map the image plane and lifted points back to 3D space based on the camera position. By predicting forward and backward lifting distances, we can form an almost closed Gaussian points distribution and reconstruct the head as completely as possible. This approach leverages the fine-grained features of the input image and significantly reduces the difficulty of predicting 3D Gaussian positions. We also utilize priors from 3D Morphable Models (3DMM) [Li et al., 2017] to further constrain the lifting distance, helping the model obtain correct 3D lifting and capture details from the source image. We then bind learnable features to the 3DMM vertices and construct expression Gaussians using image global features, 3DMM learnable features, and 3DMM point positions to ensure expression control capability. Finally, we use a neural renderer to refine the splatting-rendered results, producing the final reenacted image. Our model is learned from a large number of monocular portrait images and can be generalized to unseen identities after training. Experiments verify that our method performs better than previous methods in terms of reconstruction quality and expression accuracy, and achieves real-time reenactment and rendering speed.

Our major contributions can be summarized as follows:

- We propose GAGAvatar, which to our knowledge is the first generalizable 3D Gaussian head avatar framework that achieves single forward reconstruction and real-time reenactment.
- To achieve this, we propose a dual-lifting method to lift Gaussians from a single image and introduce a method that uses 3DMM priors to constrain the lifting process.
- We combine 3DMM priors and 3D Gaussians to accurately transfer expression information while avoiding redundant computations.

2 Related Work

2.1 2D-based Talking Head Synthesis

The impressive performance of CNN and Generative Adversarial Networks (GAN) [Goodfellow et al., 2014, Isola et al., 2017, Karras et al., 2020] has inspired many methods for direct head image synthesis using 2D networks. A popular strategy of early works is inserting the expression and head pose features of the driving image into the 2D generative network to achieve realistic and animatable image generation. For example, these methods [Zakharov et al., 2019, Burkov et al., 2020, Zhou et al., 2021, Wang et al., 2023] inject latent representations of expression into the U-Net backbone or StyleGAN-like [Karras et al., 2019] generators to transfer driving expressions to reenacted images. A recent trend in 2D-based talking head synthesis methods [Siarohin et al., 2019, Ren et al., 2021, Drobyshev et al., 2022, Hong et al., 2022a, Zhang et al., 2023a] is to represent expressions and head poses as warp fields, performing expression transfer by deforming the source image to match the driving image. However, due to the lack of explicit understanding of the 3D geometry of head portraits, these methods often produce unrealistic distortions and undesired identity changes when there are significant pose and expression variations. Although some methods [Drobyshev et al., 2022, Wang et al., 2021a, Ren et al., 2021, Yin et al., 2022, Zhang et al., 2023b] introduce 3D Morphable Models (3DMM) [Blanz and Vetter, 1999, Paysan et al., 2009, Li et al., 2017, Gerig et al., 2018]

into the 2D framework, they still lack the ability to control the viewpoint and achieve free-viewpoint rendering. Additionally, there are some audio-driven 2D control methods [Guo et al., 2021, Tang et al., 2022, Zhang et al., 2023b], while flexible to use, cannot explicitly control facial expressions and poses, sometimes resulting in unsatisfactory outcomes. In contrast, our method uses an explicit 3D representation to enable free view control and realistic synthesis even under large pose variations.

2.2 3D-based Head Avatar Reconstruction

To achieve better 3D consistency in head avatars, many works have explored using 3D representations for reconstruction. Early methods [Xu et al., 2020, Khakhulin et al., 2022] used 3DMM-based meshes [Li et al., 2017, Gerig et al., 2018] to reconstruct head avatars. Since neural radiance fields (NeRF) [Mildenhall et al., 2020] have demonstrated excellent results, many recent methods [Li et al., 2023b,a, Ma et al., 2023, Yu et al., 2023, Chu et al., 2024, Ye et al., 2024, Deng et al., 2024b,a, Park et al., 2021a, Zheng et al., 2023, Bai et al., 2023a, Ki et al., 2024] have adopted NeRF for head reconstruction. However, some approaches [Gafni et al., 2021, Park et al., 2021a, Tretschk et al., 2021, Hong et al., 2022b, Athar et al., 2022, Park et al., 2021b, Gao et al., 2022, Guo et al., 2021, Bai et al., 2023b, Kirschstein et al., 2023, Zheng et al., 2023, Bai et al., 2023a, Zhao et al., 2023, Zhang et al., 2024] require multi-view or single-view videos of specific identities for training, limiting generalization and raising privacy concerns due to the need for thousands of frames of personal image data. Additionally, some methods [Xu et al., 2023a, Tang et al., 2023, Sun et al., 2022, Xu et al., 2023b, Zhuang et al., 2022a, Sun et al., 2023] train generators to produce controllable head avatars from random noise, followed by inversion [Roich et al., 2022, Xie et al., 2023] for identity-specific reconstruction. These methods often suffer from inversion accuracy limitations, failing to preserve the identity of the source image. There are also methods [Hong et al., 2022b, Zhuang et al., 2022b, Ma et al., 2023] to perform test-time optimization on the source image to obtain reconstructions, but the need for test-time optimization limits their applicability. To address these challenges, some works [Yu et al., 2023, Li et al., 2023a,b, Ma et al., 2024a, Yang et al., 2024, Chu et al., 2024, Ye et al., 2024, Ma et al., 2024a, Deng et al., 2024b,a] focus on one-shot head reconstruction without test-time optimization. For example, GOHA [Li et al., 2023a] learns three tri-plane features to capture details. HideNeRF [Li et al., 2023b] utilizes multi-resolution tri-planes and a deformation field to generate reenactment images. GPAvatar [Chu et al., 2024] uses a point-based expression field and a multi tri-plane attention module to reconstruct head avatars. Real3DPortrait [Ye et al., 2024] generates a tri-plane from images and adds motion adapters to get reenactment images. CVTHead [Ma et al., 2024a] reconstructs head avatars using point-based neural rendering and a vertex-feature transformer. Portrait4D [Deng et al., 2024b] learns dynamic expression tri-plane from multi-view synthetic data, while Portrait4D-v2 [Deng et al., 2024a] learns from pseudo multi-view videos, addressing the lack of real video training in Portrait4D. However, these NeRF-based methods often face rendering speed limitations, preventing real-time application. Methods [Xu et al., 2024, Li et al., 2024, Hu et al., 2023, Wang et al., 2024a, Ma et al., 2024b, Wang et al., 2024b] utilizing 3D Gaussian splatting[Kerbl et al., 2023] achieve excellent performance and rendering speed but require video data for identity-specific training, lacking generalization capabilities. In this paper, we propose a one-shot 3D Gaussian head avatar reconstruction method based on the dual-lifting method. Our method can generalize to unseen identities, achieves real-time rendering, and surpasses previous works in image quality.

3 Method

An overview of the reenactment process of our method is shown in Fig. 2. Given a source image I_s, we first use DINOv2 [Darcet et al., 2023, Oquab et al., 2023] to extract global and local features. Using the local features, we apply our proposed dual-lifting methods to predict the parameters and positions of two 3D Gaussians. Simultaneously, we assign learnable parameters to each vertex of the 3DMM [Li et al., 2017] model and predict another expression Gaussians using the combination of the global feature and vertex features. We directly use the vertex positions of the 3DMM model as the positions for expression Gaussians. Finally, we combine these 3D Gaussians and perform splatting to produce a coarse result image I_c with the expression and pose of driving image I_d, which is then further refined through a neural renderer to obtain the fine result image I_f.

In the following subsections, we describe the reconstruction branch based on dual-lifting in Sec. 3.1, explain the expression modeling and control branch in Sec. 3.2, and detail our neural renderer in Sec. 3.3. Finally, we describe our lifting distance loss and the training objectives in Sec. 3.4.

https://doi.org/10.52202/079017-1838

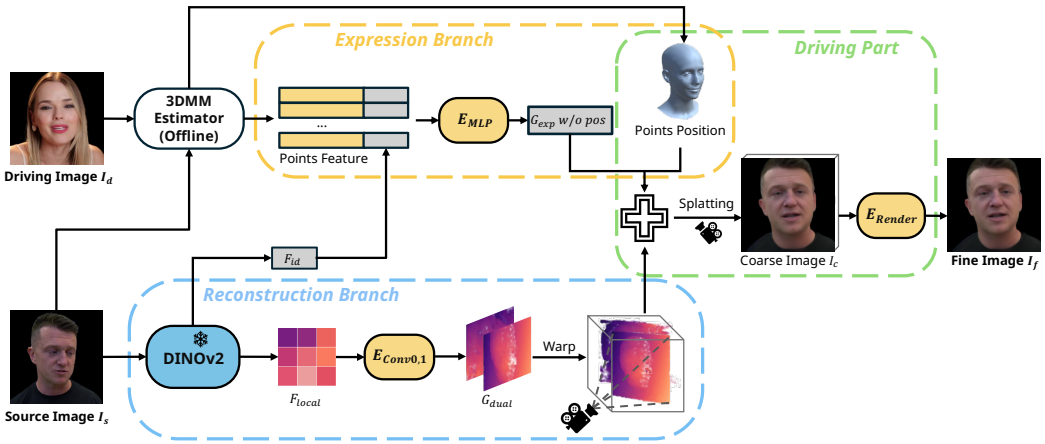

Figure 2: Our method consists of two branches: a reconstruction branch (Sec. 3.1) and an expression branch (Sec. 3.2). We render dual-lifting and expressed Gaussians to get coarse results, and then use a neural renderer to get fine results. Only a small driving part needs to be run repeatedly to drive the expression, while the rest is executed only once.

3.1 Dual-lifting and Reconstruction Branch

Given an input source image, our goal is to reconstruct a detailed 3D head avatar. To ensure stable modeling and learning, we impose certain constraints on the reconstruction process. First, we assume that the reconstructed head is always located at the origin in normalized 3D space. Second, the rotation of the head is modeled through changes in camera pose to ensure that the head itself is relatively stationary. We follow the same strategy when tracking 3DMM parameters and camera parameters from training and testing data. These constraints allow the model to effectively utilize the stable priors of the human head topology.

Leveraging the success of 3D Gaussians splatting [Kerbl et al., 2023] in synthesis quality and rendering speed, we propose a dual-lifting method to reconstruct 3D Gaussians from a single image. Reconstructing 3D Gaussians typically requires millions of points, but obtaining such a dense density of Gaussian points from a single image is a challenging task, especially without test-time optimization. To address this problem, we propose a novel reconstruction method: the dual-lifting method. Briefly, we first get the local feature plane F_{local} by a frozen DINOv2 backbone, and then predict the offsets of each pixel relative to the feature plane and the other necessary parameters (including color, opacity, scale and rotation), instead of predicting the 3D Gaussians directly. We then map the plane back to 3D space based on the camera pose and place the plane through the origin, which provides the 3D position and normal vector of the plane pixels. Finally, we can calculate the position of these 3D Gaussians in 3D space based on the predicted offsets, positions and normal vector. This process can be described as follows:

$$G_{pos} = [p_s + E_{Conv0}(F_{local}) \cdot n_s, \quad p_s - E_{Conv1}(F_{local}) \cdot n_s], \tag{1}$$

$$G_{c,o,s,r} = [E_{Conv0}(F_{local}), \quad E_{Conv1}(F_{local})], \tag{2}$$

where p_i is the initial points plane mapped based on the estimated camera pose of I_s and passes through the origin. The size of p_i is 296×296, which is consistent with the local feature F_{local}. $E_{Conv0,1}$ are convolutional networks, n_s is the normal vector of p_s, G_{pos} is the position of reconstructed 3D Gaussians, and $G_{c,o,s,r}$ represents the color, opacity, scale, and rotation of 3D Gaussians.

It's worth noting that while predicting one set of lifting distances from the plane is possible, we adopted a strategy of predicting forward and backward lifting separately. Our dual-lifting method aims to predict a complete 3D structure from a single source image, to achieve multi-view consistency during inference. If we predict only one set of lifting distances from the image plane, we may face some ambiguous situations during learning. For example, when we want to reconstruct a side view source image, predicting one set of lifting will simultaneously lift the point forward to the visible surface and backward to include the other side of the head. During this process, each pixel can be lifted to the visible surface or to the opposite surface, as both are justified, resulting in model

performance degradation. Unlike single-lifting prediction, our dual-lifting strategy predicts forward and backward lifting separately, which eliminates ambiguities and stabilizes the optimization process.

Our dual-lifting method effectively exploits the detailed information of the source image to reconstruct 3D Gaussians. At the same time, the two sets of predicted lifting points can form an almost closed Gaussian points distribution, thus enhancing the performance of large viewpoint changes. The 3D Gaussian generated by dual-lifting can be rendered from any viewpoint, producing static results. In the next section, we describe how to control the facial expressions of the generated avatar.

3.2 Expression Branch

Expression transfer is not a straightforward task, but the 3DMM [Li et al., 2017] provides us with a powerful tool to represent common facial expressions and decouple expressions from identity, thereby facilitating expression control. Our expression branch establishes 3D Gaussians based on the 3DMM vertices to control the expressions of the generated images. To achieve this, we bind learnable weights to each vertex in the 3DMM. Due to the stable semantics of 3DMM vertices, the features of these points correspond to facial positions such as the eyes and mouth.

As shown in Fig. 2, given the source image I_s and driving image I_d, we concatenate the global features F_{id} with the learnable features of vertices. We then use a MLP to predict the Gaussian parameters (excluding position) of each point from these features, and use the position of the 3DMM vertices. Here we combine the global features F_{id} of the source image when predicting the expression Gaussians. This will introduce identity information to the expression branch and enhance the identity consistency under various expressions, as confirmed by our experiments. Throughout the driving process, we only need to infer the Gaussians of the reconstruction branch and expression branch once. Reenactment is achieved by modifying the camera pose and position of the Gaussians in the expression branch, which allows us to perform fast reenactment without redundant calculations.

3.3 Neural Renderer

Reconstructing 3D Gaussians typically requires millions of points, but in our dual-lifting method, we generate only 175,232 points. These Gaussians can reconstruct the target avatar, but with RGB information alone it is insufficient for capturing the rich details of a human avatar. To enhance the representation capability of the sparse Gaussians, we predict 32-dimensional features containing RGB information and then perform splatting to obtain coarse images. Then we use a popular neural renderer following existing methods [Li et al., 2023a, Chu et al., 2024, Ye et al., 2024] to get the fine image, as Fig. 2 shows. Unlike these methods which use neural render as a super-resolution module to reduce rendering time, we do not upsample the image as our method do not face significant rendering time issues. Our neural renderer effectively decodes the dual lifting and expression Gaussians features into RGB values, producing high-quality results and resolving potential conflicts between the two sets of Gaussians. We train our neural renderer from scratch during the training process, without any pre-trained initialization.

3.4 Training Strategy and Loss Functions

With the exception of the frozen DINOv2 backbone, we train the model from scratch. During training, we randomly sample two images from the same video, one as the source image and the other as the driving image and target image. Our primary objective during training is to ensure that the reenacted coarse and fine image aligns with the target image. Given that both images share the same identity, this alignment is achievable. We employ L1 loss and perceptual loss [Johnson et al., 2016, Zhang et al., 2018, Ye et al., 2024] on both the coarse and the fine image.

Additionally, we propose a lifting distance loss $\mathcal{L}_{lifting}$ to assist dual-lifting learning. With the help of the prior provided by the tracked 3DMM, we require the lifting distance predicted by the network to be as close as possible to the 3DMM vertices. Specifically, we look for the lifting point closest to each 3DMM vertex and constrain their distance through L2 loss. The calculation is as follows:

$$\mathcal{L}_{lifting} = ||P_{3dmm} - \left\{ argmin_{q \in G_{pos}} \|p - q\| \mid p \in P_{3dmm} \right\}||, \tag{3}$$

where the P_{3dmm} is the tracked 3DMM vertices, G_{pos} is the dual-lifting points, $argmin$ find the nearest point. Our lifting distance loss leverages 3DMM priors. Additionally, since we constrain only

https://doi.org/10.52202/079017-1838

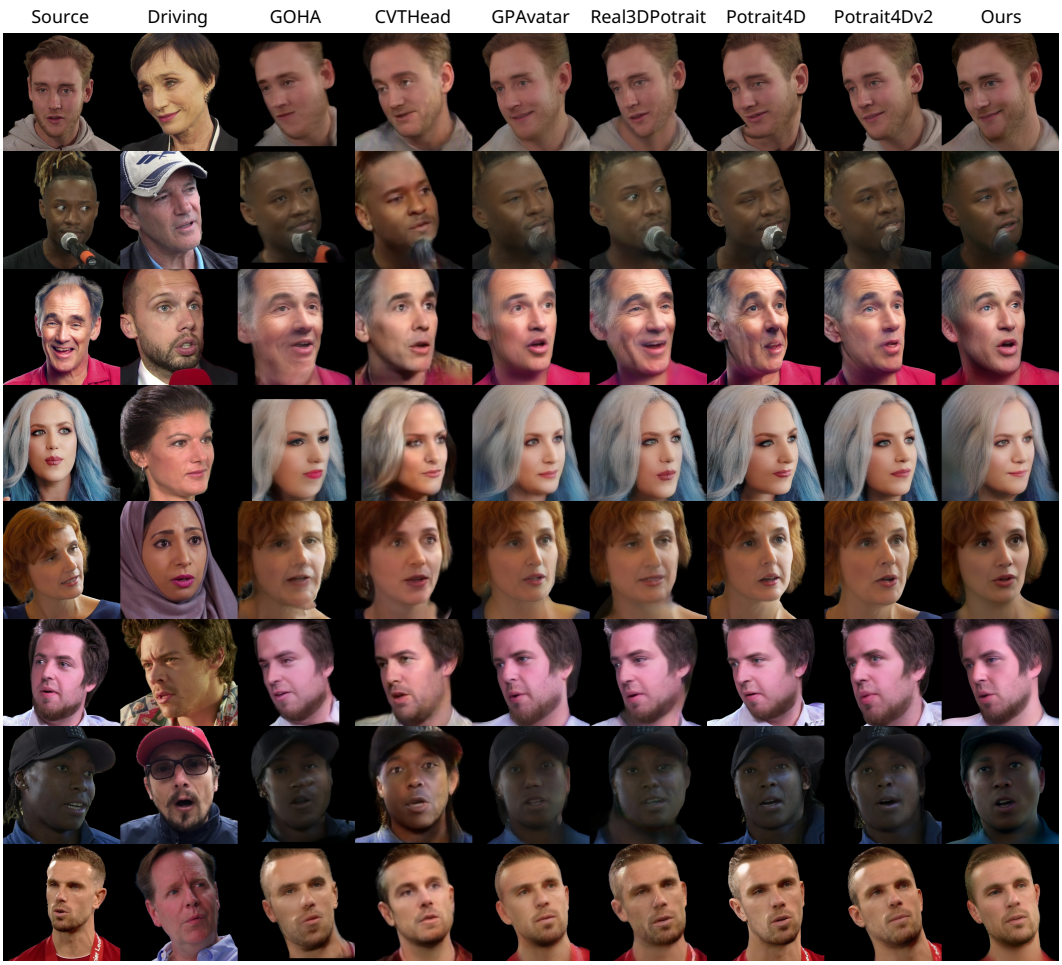

Figure 3: Cross-identity qualitative results on the VFHQ [Xie et al., 2022] dataset. Compared with baseline methods, our method has accurate expressions and rich details.

a subset of dual-lifting points, the model can still learn areas not modeled by 3DMM, such as hair and accessories. Experiments show $\mathcal{L}_{lifting}$ can improve the 3D structure and the performance of large view changes.

The overall training objective is as follows:

$$\mathcal{L} = ||I_c - I_t|| + ||I_f - I_t|| + \lambda_p(||\varphi(I_c) - \varphi(I_t)|| + ||\varphi(I_f) - \varphi(I_t)||) + \lambda_l \mathcal{L}_{lifting}, \quad (4)$$

where I_t is target image, I_c and I_f are the generated coarse and fine image, λ_p and λ_l are the weights used to balance the losses.

4 Experiments

4.1 Experiment Setting

Datasets. We use the VFHQ [Xie et al., 2022] dataset to train our model, which comprises clips from various interview scenarios. To avoid consecutive similar frames, we sampled 25 to 75 frames from the original video depending on video length. This resulted in a dataset that includes 586,382 frames from 15,204 video clips. All the images are resized to 512×512. We tracked camera poses, FLAME [Li et al., 2017] parameters and removed the background following [Chu et al., 2024]. For evaluation, we use sampled frames from the VFHQ original test split, consisting of 5000 frames from 100 videos. The first frame of each video serves as the source image, with the remaining frames used

Table 1: Quantitative results on the VFHQ [Xie et al., 2022] dataset. We use colors to denote the first, second and third places respectively.

Method	Self Reenactment							Cross Reenactment		
	PSNR↑	SSIM↑	LPIPS↓	CSIM↑	AED↓	APD↓	AKD↓	CSIM↑	AED↓	APD↓
StyleHeat [Yin et al., 2022]	19.95	0.726	0.211	0.537	0.199	0.385	7.659	0.407	0.279	0.551
ROME [Khakhulin et al., 2022]	19.96	0.786	0.192	0.701	0.138	0.186	4.986	0.530	0.259	0.277
OTAvatar [Ma et al., 2023]	17.65	0.563	0.294	0.465	0.234	0.545	18.19	0.364	0.324	0.678
HideNeRF [Li et al., 2023b]	19.79	0.768	0.180	0.787	0.143	0.361	7.254	0.514	0.277	0.527
GOHA [Li et al., 2023a]	20.15	0.770	0.149	0.664	0.176	0.173	6.272	0.518	0.274	0.261
CVTHead [Ma et al., 2024a]	18.43	0.706	0.317	0.504	0.186	0.224	5.678	0.374	0.261	0.311
GPAvatar [Chu et al., 2024]	21.04	0.807	0.150	0.772	0.132	0.189	4.226	0.564	0.255	0.328
Real3DPortrait [Ye et al., 2024]	20.88	0.780	0.154	0.801	0.150	0.268	5.971	0.663	0.296	0.411
Portrait4D [Deng et al., 2024b]	20.35	0.741	0.191	0.765	0.144	0.205	4.854	0.596	0.286	0.258
Portrait4D-v2 [Deng et al., 2024a]	21.34	0.791	0.144	0.803	0.117	0.187	3.749	0.656	0.268	0.273
Ours	21.83	0.818	0.122	0.816	0.111	0.135	3.349	0.633	0.253	0.247

Table 2: Quantitative results on the HDTF [Zhang et al., 2021] dataset. We use colors to denote the first, second and third places respectively.

Method	Self Reenactment							Cross Reenactment		
	PSNR↑	SSIM↑	LPIPS↓	CSIM↑	AED↓	APD↓	AKD↓	CSIM↑	AED↓	APD↓
StyleHeat [Yin et al., 2022]	21.41	0.785	0.155	0.657	0.158	0.162	4.585	0.632	0.271	0.239
ROME [Khakhulin et al., 2022]	20.51	0.803	0.145	0.738	0.133	0.123	4.763	0.726	0.268	0.191
OTAvatar [Ma et al., 2023]	20.52	0.696	0.166	0.662	0.180	0.170	8.295	0.643	0.292	0.222
HideNeRF [Li et al., 2023b]	21.08	0.811	0.117	0.858	0.120	0.247	5.837	0.843	0.276	0.288
GOHA [Li et al., 2023a]	21.31	0.807	0.113	0.725	0.162	0.117	6.332	0.735	0.277	0.136
CVTHead [Ma et al., 2024a]	20.08	0.762	0.179	0.608	0.169	0.138	4.585	0.591	0.242	0.203
GPAvatar [Chu et al., 2024]	23.06	0.855	0.104	0.855	0.114	0.135	3.293	0.842	0.268	0.219
Real3DPortrait [Ye et al., 2024]	22.82	0.835	0.103	0.851	0.138	0.137	4.640	0.903	0.299	0.238
Portrait4D [Deng et al., 2024b]	20.81	0.786	0.137	0.810	0.134	0.131	4.151	0.793	0.291	0.240
Portrait4D-v2 [Deng et al., 2024a]	22.87	0.860	0.105	0.860	0.111	0.111	3.292	0.857	0.262	0.183
Ours	23.13	0.863	0.103	0.862	0.110	0.111	2.985	0.851	0.231	0.181

as driving and target images for reenactment. We also evaluate on HDTF [Zhang et al., 2021] dataset, following the test split used in [Ma et al., 2023, Li et al., 2023a], including 19 video clips.

Implementation details. Our framework is built on the PyTorch [Paszke et al., 2017] platform. We use FLAME [Li et al., 2017] as our driving 3DMM. During training, we use the ADAM [Kingma and Ba, 2014] optimizer with a learning rate of 1.0e-4. The DINOv2 [Oquab et al., 2023] backbone is frozen during training and is not trained or fine-tuned. Our training consists of 200,000 iterations with a total batch size of 8. The training process is conducted on an NVIDIA Tesla A100 GPU and takes approximately 46 GPU hours, demonstrating efficient resource utilization. During inference, our method achieves 67 FPS on an A100 GPU while using only 2.5 GB of VRAM, showcasing high efficiency. Further implementation details of the model can be found in the supplementary materials.

4.2 Main Results

Baseline methods. We conduct comparisons with existing state-of-the-art methods, including ROME [Khakhulin et al., 2022], StyleHeat [Yin et al., 2022], OTAvatar [Ma et al., 2023], HideNeRF [Li et al., 2023b], GOHA [Li et al., 2023a], CVTHead [Ma et al., 2024a], GPAvatar [Chu et al., 2024], Real3DPortrait [Ye et al., 2024], Portrait4D [Deng et al., 2024b], and Portrait4D-v2 [Deng et al., 2024a]. For each method, we use the official implementation to obtain the result. It is worth noting that actually the core contributions of Portrait4D-v2 are orthogonal to our work. They introduced a new data generation method and a novel learning paradigm to improve performance, which means our method can also benefit from their advancements.

Qualitative results. Fig. 3 shows qualitative comparisons between methods. Compared with other methods, our method can reconstruct detailed head avatars from source images and capture subtle facial movements such as eyes and mouth in driving images. Our method can also maintain identity

https://doi.org/10.52202/079017-1838

Figure 4: Ablation results on VFHQ [Xie et al., 2022] datasets. We can see that our full method performs best, especially on facial edges such as glasses in large view angles.

consistency and image quality when handling large head rotations. At the same time, our method achieves high-quality reconstruction and rendering at a much faster speed than the baseline method.

Quantitative results. We also quantitatively evaluate the self and cross-identity reenactment performance between methods. For self-reenactment with ground truth available, we measure the quality of the synthesized images using PSNR, SSIM, LPIPS [Zhang et al., 2018] between the synthetic results and the ground truth. For identity similarity, we calculate the cosine distance of face recognition features [Deng et al., 2019a] between the reenactment results and the source images. For expression and pose, we use the average expression distance (AED) and average pose distance (APD) measured by a 3DMM estimator [Deng et al., 2019b], and the average keypoint distance (AKD) based on a facial landmark detector [Bulat and Tzimiropoulos, 2017] to evaluate the accuracy of driving control. For the cross-identity reenactment task, due to the lack of ground truth, we evaluate CSIM, AED, and APD, generally consistent with previous work [Li et al., 2023a, Chu et al., 2024, Ye et al., 2024].

Tab. 1 and Tab. 2 show the quantitative results on the VFHQ and HDTF datasets, respectively. Our method outperforms previous methods in terms of reconstruction and synthesis quality and expression control accuracy but the cross-reenactment identity consistency is slightly worse than some existing methods. We believe this is due to the 3DMM [Li et al., 2017] and 3DMM tracker we rely on, whose identity parameters and expression parameters are not completely decoupled. Some methods [Deng et al., 2024b,a] that are not based on 3DMM have brought some inspiration to solve this limitation, and we leave these to future work. Importantly, our model not only achieves these quantitative results, but also achieves the real-time reenactment speed, which is much faster than existing methods.

Inference speed and efficiency. Our method can run at 67 FPS on an A100 GPU with the naive PyTorch framework and official 3D Gaussian Splatting implementation. As shown in Tab. 3, we are the first real-time method for animatable one-shot head avatar reconstruction, which shows the application prospects and unique value of our method.

Table 3: The time of reenactment is measured in FPS. All results exclude the time for getting driving parameters that can be calculated in advance and are averaged over 100 frames.

	StyleHeat	ROME	OTAvatar	HideNeRF	GOHA	CVTHead	GPAvatar	Real3D	P4D	P4D-v2	Ours
Driving FPS	19.82	11.21	0.12	9.73	6.57	18.09	16.86	4.55	9.49	9.62	67.12

4.3 Ablation Studies

Dual-lifting. To validate the effectiveness of our proposed dual-lifting method, we compare it against a baseline that lifts points from a single plane. This baseline requires the model to simultaneously lift points forward and backward from the image plane, sometimes creating ambiguities. The results in Tab. 4 and Fig. 4 show that dual-lifting significantly enhances reconstruction quality. Moreover, since the lifting is performed only once per identity and subsequent expression driving does not require recalculation, dual-lifting does not impact the performance during reenactment.

Table 4: Ablation results on the VFHQ [Xie et al., 2022] dataset.

Method	Self Reenactment							Cross Reenactment		
	PSNR↑	SSIM↑	LPIPS↓	CSIM↑	AED↓	APD↓	AKD↓	CSIM↑	AED↓	APD↓
one-plane lifting	21.34	0.802	0.158	0.781	0.127	0.170	3.810	0.581	0.272	0.290
w/o F_{id}	21.13	0.807	0.155	0.774	0.125	0.155	3.722	0.537	0.270	0.272
w/o neural renderer	20.34	0.789	0.138	0.788	0.147	0.202	4.763	0.623	0.300	0.353
w/o $\mathcal{L}_{lifting}$	21.64	0.812	0.148	0.800	0.119	0.151	3.563	0.620	0.261	0.252
Ours	21.83	0.818	0.122	0.816	0.111	0.135	3.349	0.633	0.253	0.247

Figure 5: Lifting results of an in-the-wild image, include the front view and the top view. Points are filtered by Gaussian opacity. We color two parts of the dual-lifting separately, and the black points are the image plane. It can be seen that the lifted 3D structure is relatively flat without $\mathcal{L}_{lifting}$.

Lifting distance loss. We evaluate the influence of the lifting distance loss $\mathcal{L}_{lifting}$ by removing it during training. Without lifting distance loss, we observed performance degradation as shown in Tab. 4 and Fig. 4. Compared with our full method, removing the point distance constraint will make it more difficult to reconstruct high-quality 3D structures, especially on facial edges.

3D structure of dual-lifting. We further analyze and compare the 3D structure of dual-lifting. We show the visualization of filtered lifting points in Fig. 5. It can be seen that in the case of single-plane lifting or without $\mathcal{L}_{lifting}$, the model can learn the correct 3D lifting even without any explicit 3D constraints. However, dual-lifting can produce 3D Gaussian points away from the input angle, and the 3D structure is also more reasonable rather than relatively flat.

Global feature in expression branch. We conduct an ablation study by removing the global identity features F_{id} from the expression branch. The results in Tab. 4 and Fig. 4 indicate that removing F_{id} decreases the identity similarity (CSIM) of the results and the reenactment quality. This demonstrates the importance of incorporating identity information in the expression branch.

Neural renderer. Due to the sparsity of our reconstructed Gaussians, we increased the output dimensions and introduced a neural renderer to refine the coarse images and features. This process is similar to the super-resolution module in EG3D [Chan et al., 2022], but our neural renderer does not increase the resolution of the results. The results in Tab. 4 and Fig. 4 show the performance of coarse results without neural rendering. It can be observed that we can obtain reasonable results even using only sparse Gaussians, but the neural renderer significantly improves detail and expression.

Extreme inputs. We present more qualitative results with extreme inputs in Fig. 6. For extreme expressions or common occlusions such as sunglasses, our method shows good robustness. Our model can also work well with low-quality images and challenging lighting conditions, but the details of reconstructed avatars are inevitably affected. For example, avatars reconstructed from blurred images lack details, while those from images with challenging lighting conditions have fixed lighting, such as shadows on the nose. However, these features also demonstrate that our method can faithfully restore details and handle various extreme cases.

Resolve conflicts of dual-lifting and expression Gaussians. Although we attempt to bring the two sets of Gaussians closer, there are inherent conflicts since one set is static and the other is dynamic. We show some results with conflicts in Fig. 7. It can be seen that the RGB values conflict when there is a significant expression difference between the dual-lifting Gaussians and the expression Gaussians, but these conflicts are well resolved after neural rendering. We believe this is because our Gaussians have 32-D features that contain more information than RGB values. The neural rendering module can act as a filter to integrate the two point sets using these features and resolving possible conflicts.

https://doi.org/10.52202/079017-1838

Figure 6: The robustness of our model. Our method can produce reasonable results for low-quality images, challenging lighting conditions, significant occlusions, and extreme expressions.

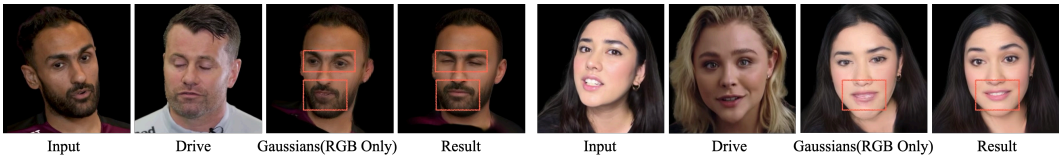

Figure 7: The case where two sets of Gaussians conflict, the conflict is resolved after neural rendering. We believe that neural rendering resolves the conflict through the 32D features carried by Gaussians.

5 Conclusion

In this paper, we proposed a novel framework for one-shot head avatar reconstruction and real-time reenactment. The key innovation of our method is the dual-lifting approach for one-shot 3D Gaussian reconstruction, which estimates the Gaussian parameters in a single forward pass. We also propose a 3DMM-based expression control method and a loss function that uses 3DMM priors to constrain the lifting process. Our experiments demonstrate that our method outperforms state-of-the-art baselines in both the quality of head avatar reconstruction and reenactment accuracy, with significant improvements in rendering speed. We believe our method has a wide range of potential applications due to its strong generalization capabilities and real-time rendering speed.

Broader impacts. Although our method has great potential in various applications, it also poses the risk of misuse, such as generating fake videos and spreading false information. We strongly oppose such misuse and have proposed several measures to prevent it, as detailed in Sec. E. With proper and responsible use, we believe our method can offer significant benefits in a wide range of applications such as video conferencing and entertainment industries.

Limitations and future work. Despite its strengths, our method has certain limitations. For example our model may generate less detail for unseen areas, and our 3DMM-based expression branch cannot control the areas not modeled by 3DMM, such as hair and tongue. These limitations highlight the possible improvements in future work to increase the performance and practicality of our method. In Sec. F, we provide a more detailed discussion of our limitations and future work.

Acknowledgements

This work was partially supported by JST Moonshot R&D Grant Number JPMJPS2011, CREST Grant Number JPMJCR2015 and Basic Research Grant (Super AI) of Institute for AI and Beyond of the University of Tokyo. In addition, this work was also partially supported by JST SPRING, Grant Number JPMJSP2108.

References

Fei Yin, Yong Zhang, Xiaodong Cun, Mingdeng Cao, Yanbo Fan, Xuan Wang, Qingyan Bai, Baoyuan Wu, Jue Wang, and Yujiu Yang. Styleheat: One-shot high-resolution editable talking face generation via pre-trained stylegan. In *European Conference on Computer Vision (ECCV)*, 2022.

Yurui Ren, Ge Li, Yuanqi Chen, Thomas H Li, and Shan Liu. Pirenderer: Controllable portrait image generation via semantic neural rendering. In *IEEE International Conference on Computer Vision (ICCV)*, 2021.

Ben Mildenhall, Pratul P. Srinivasan, Matthew Tancik, Jonathan T. Barron, Ravi Ramamoorthi, and Ren Ng. Nerf: Representing scenes as neural radiance fields for view synthesis. In *ECCV*, 2020.

Zhiyuan Ma, Xiangyu Zhu, Guojun Qi, Zhen Lei, and Lei Zhang. Otavatar: One-shot talking face avatar with controllable tri-plane rendering. In *IEEE Conference on Computer Vision and Pattern Recognition (CVPR)*, 2023.

Xueting Li, Shalini De Mello, Sifei Liu, Koki Nagano, Umar Iqbal, and Jan Kautz. Generalizable one-shot neural head avatar. *Arxiv*, 2023a.

Xuangeng Chu, Yu Li, Ailing Zeng, Tianyu Yang, Lijian Lin, Yunfei Liu, and Tatsuya Harada. GPAvatar: Generalizable and precise head avatar from image(s). In *The Twelfth International Conference on Learning Representations*, 2024.

Yu Deng, Duomin Wang, and Baoyuan Wang. Portrait4d-v2: Pseudo multi-view data creates better 4d head synthesizer. *arXiv preprint arXiv:2403.13570*, 2024a.

Bernhard Kerbl, Georgios Kopanas, Thomas Leimkühler, and George Drettakis. 3d gaussian splatting for real-time radiance field rendering. *ACM Transactions on Graphics*, 42, 2023.

Yuelang Xu, Benwang Chen, Zhe Li, Hongwen Zhang, Lizhen Wang, Zerong Zheng, and Yebin Liu. Gaussian head avatar: Ultra high-fidelity head avatar via dynamic gaussians. In *Proceedings of the IEEE/CVF Conference on Computer Vision and Pattern Recognition (CVPR)*, 2024.

Tianye Li, Timo Bolkart, Michael. J. Black, Hao Li, and Javier Romero. Learning a model of facial shape and expression from 4D scans. *ACM Transactions on Graphics, (Proc. SIGGRAPH Asia)*, pages 194:1–194:17, 2017.

Ian Goodfellow, Jean Pouget-Abadie, Mehdi Mirza, Bing Xu, David Warde-Farley, Sherjil Ozair, Aaron Courville, and Yoshua Bengio. Generative adversarial nets. *Advances in neural information processing systems*, 27, 2014.

Phillip Isola, Jun-Yan Zhu, Tinghui Zhou, and Alexei A Efros. Image-to-image translation with conditional adversarial networks. In *Proceedings of the IEEE conference on computer vision and pattern recognition*, pages 1125–1134, 2017.

Tero Karras, Samuli Laine, Miika Aittala, Janne Hellsten, Jaakko Lehtinen, and Timo Aila. Analyzing and improving the image quality of stylegan. In *Proceedings of the IEEE/CVF conference on computer vision and pattern recognition*, pages 8110–8119, 2020.

Egor Zakharov, Aliaksandra Shysheya, Egor Burkov, and Victor Lempitsky. Few-shot adversarial learning of realistic neural talking head models. In *Proceedings of the IEEE/CVF international conference on computer vision*, pages 9459–9468, 2019.

Egor Burkov, Igor Pasechnik, Artur Grigorev, and Victor Lempitsky. Neural head reenactment with latent pose descriptors. In *Proceedings of the IEEE/CVF conference on computer vision and pattern recognition*, pages 13786–13795, 2020.

Hang Zhou, Yasheng Sun, Wayne Wu, Chen Change Loy, Xiaogang Wang, and Ziwei Liu. Pose-controllable talking face generation by implicitly modularized audio-visual representation. In *Proceedings of the IEEE/CVF conference on computer vision and pattern recognition*, pages 4176–4186, 2021.

 https://doi.org/10.52202/079017-1838

Duomin Wang, Yu Deng, Zixin Yin, Heung-Yeung Shum, and Baoyuan Wang. Progressive disentangled representation learning for fine-grained controllable talking head synthesis. In *Proceedings of the IEEE/CVF Conference on Computer Vision and Pattern Recognition*, pages 17979–17989, 2023.

Tero Karras, Samuli Laine, and Timo Aila. A style-based generator architecture for generative adversarial networks. In *Proceedings of the IEEE/CVF conference on computer vision and pattern recognition*, pages 4401–4410, 2019.

Aliaksandr Siarohin, Stéphane Lathuilière, Sergey Tulyakov, Elisa Ricci, and Nicu Sebe. First order motion model for image animation. *Advances in neural information processing systems*, 32, 2019.

Nikita Drobyshev, Jenya Chelishev, Taras Khakhulin, Aleksei Ivakhnenko, Victor Lempitsky, and Egor Zakharov. Megaportraits: One-shot megapixel neural head avatars. In *Proceedings of the 30th ACM International Conference on Multimedia*, pages 2663–2671, 2022.

Fa-Ting Hong, Longhao Zhang, Li Shen, and Dan Xu. Depth-aware generative adversarial network for talking head video generation. In *Proceedings of the IEEE/CVF conference on computer vision and pattern recognition*, pages 3397–3406, 2022a.

Bowen Zhang, Chenyang Qi, Pan Zhang, Bo Zhang, HsiangTao Wu, Dong Chen, Qifeng Chen, Yong Wang, and Fang Wen. Metaportrait: Identity-preserving talking head generation with fast personalized adaptation. In *Proceedings of the IEEE/CVF Conference on Computer Vision and Pattern Recognition*, pages 22096–22105, 2023a.

Ting-Chun Wang, Arun Mallya, and Ming-Yu Liu. One-shot free-view neural talking-head synthesis for video conferencing. In *Proceedings of the IEEE/CVF conference on computer vision and pattern recognition*, pages 10039–10049, 2021a.

Wenxuan Zhang, Xiaodong Cun, Xuan Wang, Yong Zhang, Xi Shen, Yu Guo, Ying Shan, and Fei Wang. Sadtalker: Learning realistic 3d motion coefficients for stylized audio-driven single image talking face animation. *Proceedings of the IEEE/CVF Conference on Computer Vision and Pattern Recognition*, pages 8652–8661, 2023b.

Volker Blanz and Thomas Vetter. A morphable model for the synthesis of 3d faces. In *Proceedings of the 26th annual conference on Computer graphics and interactive techniques*, 1999.

Pascal Paysan, Reinhard Knothe, Brian Amberg, Sami Romdhani, and Thomas Vetter. A 3d face model for pose and illumination invariant face recognition. In *2009 sixth IEEE international conference on advanced video and signal based surveillance*, pages 296–301, 2009.

Thomas Gerig, Andreas Morel-Forster, Clemens Blumer, Bernhard Egger, Marcel Luthi, Sandro Schönborn, and Thomas Vetter. Morphable face models-an open framework. In *2018 13th IEEE International Conference on Automatic Face & Gesture Recognition (FG 2018)*, pages 75–82, 2018.

Yudong Guo, Keyu Chen, Sen Liang, Yong-Jin Liu, Hujun Bao, and Juyong Zhang. Ad-nerf: Audio driven neural radiance fields for talking head synthesis. In *Proceedings of the IEEE/CVF International Conference on Computer Vision*, pages 5784–5794, 2021.

Jiaxiang Tang, Kaisiyuan Wang, Hang Zhou, Xiaokang Chen, Dongliang He, Tianshu Hu, Jingtuo Liu, Gang Zeng, and Jingdong Wang. Real-time neural radiance talking portrait synthesis via audio-spatial decomposition. *arXiv preprint arXiv:2211.12368*, 2022.

Sicheng Xu, Jiaolong Yang, Dong Chen, Fang Wen, Yu Deng, Yunde Jia, and Xin Tong. Deep 3d portrait from a single image. In *Proceedings of the IEEE/CVF Conference on Computer Vision and Pattern Recognition*, pages 7710–7720, 2020.

Taras Khakhulin, Vanessa Sklyarova, Victor Lempitsky, and Egor Zakharov. Realistic one-shot mesh-based head avatars. In *European Conference on Computer Vision (ECCV)*, 2022.

Weichuang Li, Longhao Zhang, Dong Wang, Bin Zhao, Zhigang Wang, Mulin Chen, Bang Zhang, Zhongjian Wang, Liefeng Bo, and Xuelong Li. One-shot high-fidelity talking-head synthesis with deformable neural radiance field. In *IEEE Conference on Computer Vision and Pattern Recognition (CVPR)*, 2023b.

Wangbo Yu, Yanbo Fan, Yong Zhang, Xuan Wang, Fei Yin, Yunpeng Bai, Yan-Pei Cao, Ying Shan, Yang Wu, Zhongqian Sun, et al. Nofa: Nerf-based one-shot facial avatar reconstruction. In *ACM SIGGRAPH 2023 Conference Proceedings*, pages 1–12, 2023.

Zhenhui Ye, Tianyun Zhong, Yi Ren, Jiaqi Yang, Weichuang Li, Jiawei Huang, Ziyue Jiang, Jinzheng He, Rongjie Huang, Jinglin Liu, et al. Real3d-portrait: One-shot realistic 3d talking portrait synthesis. *arXiv preprint arXiv:2401.08503*, 2024.

Yu Deng, Duomin Wang, Xiaohang Ren, Xingyu Chen, and Baoyuan Wang. Portrait4d: Learning one-shot 4d head avatar synthesis using synthetic data. In *IEEE/CVF Conference on Computer Vision and Pattern Recognition*, 2024b.

Keunhong Park, Utkarsh Sinha, Jonathan T. Barron, Sofien Bouaziz, Dan B Goldman, Steven M. Seitz, and Ricardo Martin-Brualla. Nerfies: Deformable neural radiance fields. *IEEE International Conference on Computer Vision (ICCV)*, 2021a.

Yufeng Zheng, Wang Yifan, Gordon Wetzstein, Michael J Black, and Otmar Hilliges. Pointavatar: Deformable point-based head avatars from videos. In *Proceedings of the IEEE/CVF conference on computer vision and pattern recognition*, pages 21057–21067, 2023.

Yunpeng Bai, Yanbo Fan, Xuan Wang, Yong Zhang, Jingxiang Sun, Chun Yuan, and Ying Shan. High-fidelity facial avatar reconstruction from monocular video with generative priors. In *Proceedings of the IEEE/CVF Conference on Computer Vision and Pattern Recognition (CVPR)*, 2023a.

Taekyung Ki, Dongchan Min, and Gyeongsu Chae. Learning to generate conditional tri-plane for 3d-aware expression controllable portrait animation. *arXiv preprint arXiv:2404.00636*, 2024.

Guy Gafni, Justus Thies, Michael Zollhofer, and Matthias Nießner. Dynamic neural radiance fields for monocular 4d facial avatar reconstruction. In *Proceedings of the IEEE/CVF Conference on Computer Vision and Pattern Recognition*, pages 8649–8658, 2021.

Edgar Tretschk, Ayush Tewari, Vladislav Golyanik, Michael Zollhöfer, Christoph Lassner, and Christian Theobalt. Non-rigid neural radiance fields: Reconstruction and novel view synthesis of a dynamic scene from monocular video. In *Proceedings of the IEEE/CVF International Conference on Computer Vision*, 2021.

Yang Hong, Bo Peng, Haiyao Xiao, Ligang Liu, and Juyong Zhang. Headnerf: A real-time nerf-based parametric head model. In *Proceedings of the IEEE/CVF Conference on Computer Vision and Pattern Recognition*, pages 20374–20384, 2022b.

ShahRukh Athar, Zexiang Xu, Kalyan Sunkavalli, Eli Shechtman, and Zhixin Shu. Rignerf: Fully controllable neural 3d portraits. In *Proceedings of the IEEE/CVF conference on Computer Vision and Pattern Recognition*, 2022.

Keunhong Park, Utkarsh Sinha, Peter Hedman, Jonathan T. Barron, Sofien Bouaziz, Dan B Goldman, Ricardo Martin-Brualla, and Steven M. Seitz. Hypernerf: A higher-dimensional representation for topologically varying neural radiance fields. *ACM Trans. Graph.*, 2021b.

Xuan Gao, Chenglai Zhong, Jun Xiang, Yang Hong, Yudong Guo, and Juyong Zhang. Reconstructing personalized semantic facial nerf models from monocular video. *ACM Transactions on Graphics (TOG)*, 41, 2022.

Ziqian Bai, Feitong Tan, Zeng Huang, Kripasindhu Sarkar, Danhang Tang, Di Qiu, Abhimitra Meka, Ruofei Du, Mingsong Dou, Sergio Orts-Escolano, et al. Learning personalized high quality volumetric head avatars from monocular rgb videos. In *Proceedings of the IEEE/CVF Conference on Computer Vision and Pattern Recognition*, 2023b.

Tobias Kirschstein, Shenhan Qian, Simon Giebenhain, Tim Walter, and Matthias Nießner. Nersemble: Multi-view radiance field reconstruction of human heads. *ACM Transactions on Graphics (TOG)*, 42, 2023.

Xiaochen Zhao, Lizhen Wang, Jingxiang Sun, Hongwen Zhang, Jinli Suo, and Yebin Liu. Havatar: High-fidelity head avatar via facial model conditioned neural radiance field. *ACM Transactions on Graphics*, 43, 2023.

 https://doi.org/10.52202/079017-1838

Zicheng Zhang, Ruobing Zheng, Ziwen Liu, Congying Han, Tianqi Li, Meng Wang, Tiande Guo, Jingdong Chen, Bonan Li, and Ming Yang. Learning dynamic tetrahedra for high-quality talking head synthesis. *arXiv preprint arXiv:2402.17364*, 2024.

Zhongcong Xu, Jianfeng Zhang, Junhao Liew, Wenqing Zhang, Song Bai, Jiashi Feng, and Mike Zheng Shou. Pv3d: A 3d generative model for portrait video generation. In *The Tenth International Conference on Learning Representations*, 2023a.

Junshu Tang, Bo Zhang, Binxin Yang, Ting Zhang, Dong Chen, Lizhuang Ma, and Fang Wen. 3dfaceshop: Explicitly controllable 3d-aware portrait generation. *IEEE Transactions on Visualization & Computer Graphics*, 2023.

Keqiang Sun, Shangzhe Wu, Zhaoyang Huang, Ning Zhang, Quan Wang, and HongSheng Li. Controllable 3d face synthesis with conditional generative occupancy fields. *Advances in Neural Information Processing Systems*, 35, 2022.

Hongyi Xu, Guoxian Song, Zihang Jiang, Jianfeng Zhang, Yichun Shi, Jing Liu, Wanchun Ma, Jiashi Feng, and Linjie Luo. Omniavatar: Geometry-guided controllable 3d head synthesis. In *Proceedings of the IEEE/CVF Conference on Computer Vision and Pattern Recognition*, pages 12814–12824, 2023b.

Peiye Zhuang, Liqian Ma, Sanmi Koyejo, and Alexander Schwing. Controllable radiance fields for dynamic face synthesis. In *2022 International Conference on 3D Vision (3DV)*, 2022a.

Jingxiang Sun, Xuan Wang, Lizhen Wang, Xiaoyu Li, Yong Zhang, Hongwen Zhang, and Yebin Liu. Next3d: Generative neural texture rasterization for 3d-aware head avatars. In *Proceedings of the IEEE/CVF conference on computer vision and pattern recognition*, 2023.

Daniel Roich, Ron Mokady, Amit H Bermano, and Daniel Cohen-Or. Pivotal tuning for latent-based editing of real images. *ACM Transactions on graphics (TOG)*, 2022.

Jiaxin Xie, Hao Ouyang, Jingtan Piao, Chenyang Lei, and Qifeng Chen. High-fidelity 3d gan inversion by pseudo-multi-view optimization. In *Proceedings of the IEEE/CVF Conference on Computer Vision and Pattern Recognition*, pages 321–331, 2023.

Yiyu Zhuang, Hao Zhu, Xusen Sun, and Xun Cao. Mofanerf: Morphable facial neural radiance field. In *European conference on computer vision*, 2022b.

Haoyu Ma, Tong Zhang, Shanlin Sun, Xiangyi Yan, Kun Han, and Xiaohui Xie. Cvthead: One-shot controllable head avatar with vertex-feature transformer. In *Proceedings of the IEEE/CVF Winter Conference on Applications of Computer Vision*, 2024a.

Songlin Yang, Wei Wang, Yushi Lan, Xiangyu Fan, Bo Peng, Lei Yang, and Jing Dong. Learning dense correspondence for nerf-based face reenactment. In *Proceedings of the AAAI Conference on Artificial Intelligence*, volume 38, 2024.

Jiahe Li, Jiawei Zhang, Xiao Bai, Jin Zheng, Xin Ning, Jun Zhou, and Lin Gu. Talkinggaussian: Structure-persistent 3d talking head synthesis via gaussian splatting. *arXiv preprint arXiv:2404.15264*, 2024.

Liangxiao Hu, Hongwen Zhang, Yuxiang Zhang, Boyao Zhou, Boning Liu, Shengping Zhang, and Liqiang Nie. Gaussianavatar: Towards realistic human avatar modeling from a single video via animatable 3d gaussians. *arXiv preprint arXiv:2312.02134*, 2023.

Cong Wang, Di Kang, He-Yi Sun, Shen-Han Qian, Zi-Xuan Wang, Linchao Bao, and Song-Hai Zhang. Mega: Hybrid mesh-gaussian head avatar for high-fidelity rendering and head editing. *arXiv preprint arXiv:2404.19026*, 2024a.

Shengjie Ma, Yanlin Weng, Tianjia Shao, and Kun Zhou. 3d gaussian blendshapes for head avatar animation. *arXiv preprint arXiv:2404.19398*, 2024b.

Shengze Wang, Xueting Li, Chao Liu, Matthew Chan, Michael Stengel, Josef Spjut, Henry Fuchs, Shalini De Mello, and Koki Nagano. Coherent 3d portrait video reconstruction via triplane fusion. *arXiv preprint arXiv:2405.00794*, 2024b.

Timothée Darcet, Maxime Oquab, Julien Mairal, and Piotr Bojanowski. Vision transformers need registers, 2023.

Maxime Oquab, Timothée Darcet, Theo Moutakanni, Huy V. Vo, Marc Szafraniec, Vasil Khalidov, Pierre Fernandez, Daniel Haziza, Francisco Massa, Alaaeldin El-Nouby, Russell Howes, Po-Yao Huang, Hu Xu, Vasu Sharma, Shang-Wen Li, Wojciech Galuba, Mike Rabbat, Mido Assran, Nicolas Ballas, Gabriel Synnaeve, Ishan Misra, Herve Jegou, Julien Mairal, Patrick Labatut, Armand Joulin, and Piotr Bojanowski. Dinov2: Learning robust visual features without supervision, 2023.

Justin Johnson, Alexandre Alahi, and Li Fei-Fei. Perceptual losses for real-time style transfer and super-resolution. In *Computer Vision–ECCV 2016: 14th European Conference, Amsterdam, The Netherlands, October 11-14, 2016, Proceedings, Part II 14*. Springer, 2016.

Richard Zhang, Phillip Isola, Alexei A Efros, Eli Shechtman, and Oliver Wang. The unreasonable effectiveness of deep features as a perceptual metric. In *Proceedings of the IEEE conference on computer vision and pattern recognition*, 2018.

Liangbin Xie, Xintao Wang, Honglun Zhang, Chao Dong, and Ying Shan. Vfhq: A high-quality dataset and benchmark for video face super-resolution. In *The IEEE Conference on Computer Vision and Pattern Recognition Workshops (CVPRW)*, 2022.

Zhimeng Zhang, Lincheng Li, Yu Ding, and Changjie Fan. Flow-guided one-shot talking face generation with a high-resolution audio-visual dataset. In *Proceedings of the IEEE/CVF Conference on Computer Vision and Pattern Recognition*, 2021.

Adam Paszke, Sam Gross, Soumith Chintala, Gregory Chanan, Edward Yang, Zachary DeVito, Zeming Lin, Alban Desmaison, Luca Antiga, and Adam Lerer. Automatic differentiation in pytorch. 2017.

Diederik P Kingma and Jimmy Ba. Adam: A method for stochastic optimization. *arXiv preprint arXiv:1412.6980*, 2014.

Jiankang Deng, Jia Guo, Niannan Xue, and Stefanos Zafeiriou. Arcface: Additive angular margin loss for deep face recognition. In *Proceedings of the IEEE/CVF conference on computer vision and pattern recognition*, 2019a.

Yu Deng, Jiaolong Yang, Sicheng Xu, Dong Chen, Yunde Jia, and Xin Tong. Accurate 3d face reconstruction with weakly-supervised learning: From single image to image set. In *Proceedings of the IEEE/CVF conference on computer vision and pattern recognition workshops*, 2019b.

Adrian Bulat and Georgios Tzimiropoulos. How far are we from solving the 2d & 3d face alignment problem?(and a dataset of 230,000 3d facial landmarks). In *Proceedings of the IEEE international conference on computer vision*, 2017.

Eric R Chan, Connor Z Lin, Matthew A Chan, Koki Nagano, Boxiao Pan, Shalini De Mello, Orazio Gallo, Leonidas J Guibas, Jonathan Tremblay, Sameh Khamis, et al. Efficient geometry-aware 3d generative adversarial networks. In *Proceedings of the IEEE/CVF Conference on Computer Vision and Pattern Recognition*, 2022.

Kaiming He, Xiangyu Zhang, Shaoqing Ren, and Jian Sun. Deep residual learning for image recognition. In *Proceedings of the IEEE conference on computer vision and pattern recognition*, pages 770–778, 2016.

Xintao Wang, Yu Li, Honglun Zhang, and Ying Shan. Towards real-world blind face restoration with generative facial prior. In *The IEEE Conference on Computer Vision and Pattern Recognition (CVPR)*, 2021b.

Matthew Tancik, Ben Mildenhall, and Ren Ng. Stegastamp: Invisible hyperlinks in physical photographs. In *Proceedings of the IEEE/CVF conference on computer vision and pattern recognition*, pages 2117–2126, 2020.

 https://doi.org/10.52202/079017-1838

A Reproducibility

A.1 More Implementation Details

Specifically, we use DINOv2 Base as our feature extractor, which takes $3 \times 518 \times 518$ images as input, and encodes 296×296 local feature maps and 768-dimensional global features. We then obtain the Gaussian parameters of each pixel through 4 groups of ResBlocks He et al. [2016] without down-sampling. The dimension of Gaussian parameters is 41 dimensions, including 32 dimensions of color information, 1 dimension of opacity information, 3 dimensions of scale information, 4 dimensions of rotation information, and 1 dimension of lifting distance information. Since FLAME [Li et al., 2017] contains 5023 points, we assign a 256-dimensional feature to each point, so the total point feature size is 5023×256. We concatenate these features with global features to predict expression Gaussian parameters using an MLP with 1024 input dimensions. This MLP contains 6 layers, and since it does not include lifting distance, the output is 40 dimensions. Our neural renderer employs StyleUNet [Wang et al., 2021b] to map images from $32 \times 512 \times 512$ to $3 \times 512 \times 512$ dimensions. We also provide the code for the model in the supplementary material for reference.

A.2 More Data Processing Details

We use 15,204 video clips from the VFHQ dataset [Xie et al., 2022] for training and 100 videos for testing, following the original VFHQ split. For training videos, we uniformly sample frames based on the video's length: 25 frames if the video is less than 2 seconds, 50 frames if the video is 2 to 3 seconds, and 75 frames if the video is longer than 3 seconds. For testing videos, we uniformly sample 50 frames from each clip, resulting in a total of frames for training and 5,000 frames for testing. For the HDTF dataset, we use the test split from OTAvatar [Ma et al., 2023], which includes 19 videos. We uniformly sample 100 frames from each video, creating a test set with 1,900 frames.

For all these frames, we remove the background and resize them to 512×512 pixels. We extract and refine the 3DMM parameters for each frame following [Chu et al., 2024]. Although the labels generated by this automatic annotation method are somewhat noisy and imperfect, this approach allows us to build a large dataset, effectively mitigating the impact of data inaccuracies.

A.3 More Evaluation Details

We conduct comparisons with several state-of-the-art methods, including ROME [Khakhulin et al., 2022], StyleHeat [Yin et al., 2022], OTAvatar [Ma et al., 2023], HideNeRF [Li et al., 2023b], GOHA [Li et al., 2023a], CVTHead [Ma et al., 2024a], GPAvatar [Chu et al., 2024], Real3DPortrait [Ye et al., 2024], Portrait4D [Deng et al., 2024b], and Portrait4D-v2 [Deng et al., 2024a]. For each method, we use the official data pre-processing script to process its input frame and driver frame, and use the official implementation to obtain the result frame. To ensure a fair comparison, we realign the results from all methods, as some methods crop and center the face region while others do not. Specifically, we detect landmarks and crop the head region at the same size for all driving images and results, and then resize the results to 512×512 for evaluation.

It is worth noting that although Portrait4D and Portrait4D-v2 achieve the same functionality and get really good results, their core contributions are orthogonal to our work. They introduce a new data generation method and a new learning paradigm, which means our method can also benefit from their advancements. We leave the integration of these parallel works to future research.

B Preliminaries of 3DMM

We utilize a widely-used 3D morphable model (3DMM): the FLAME [Li et al., 2017] model which renowned for its geometric accuracy and versatility. This model is popular in applications such as facial animation, avatar creation, and facial recognition due to its realistic rendering capabilities and flexibility. We use it to work as our expression driven signal and geometry prior. The FLAME model represents the head shape as follows:

$$TP(\hat{\beta}, \hat{\theta}, \hat{\psi}) = \bar{T} + BS(\hat{\beta}; S) + BP(\hat{\theta}; P) + BE(\hat{\psi}; E), \tag{5}$$

where $\bar{T}$ is the template head avatar mesh, $BS(\hat{\beta}; S)$ is the shape blend-shape function to account for identity-related shape variation, $BP(\hat{\theta}; P)$ is a jaw and neck pose part to correct pose deformations

Figure 8: Reenactment and multi-view results of our method on in-the-wild images. From left to right: input image, driving image, driving and novel view results.

that cannot be explained solely by linear blend skinning, and expression blend-shapes $BE(\hat{\psi}; E)$ is used to capture facial expressions such as closing eyes or smiling.

C Per-part Rendering and 3D Lifting of Our Method

We present the results of rendering the dual-lifting Gaussians from the reconstruction branch and the Gaussian from the expression branch separately. As Fig. 9 shows, the dual-lifting Gaussians

https://doi.org/10.52202/079017-1838

Figure 9: Per-part rendering of the dual-lifting and expression Gaussians. We can see that the dual-lifting Gaussians reconstruct the head's base structure and facial details respectively. It is worth noting that our Gaussians are not purely RGB Gaussians. Instead, our Gaussians include 32-D features (as described in Sec. 3.3). We visualize the first 3 dimensions of these features (i.e., the RGB values of the Gaussians) here without the neural rendering module. So this visualization is intended to intuitively display the functionality of each part and the importance of each branch should not be judged based on RGB values alone.

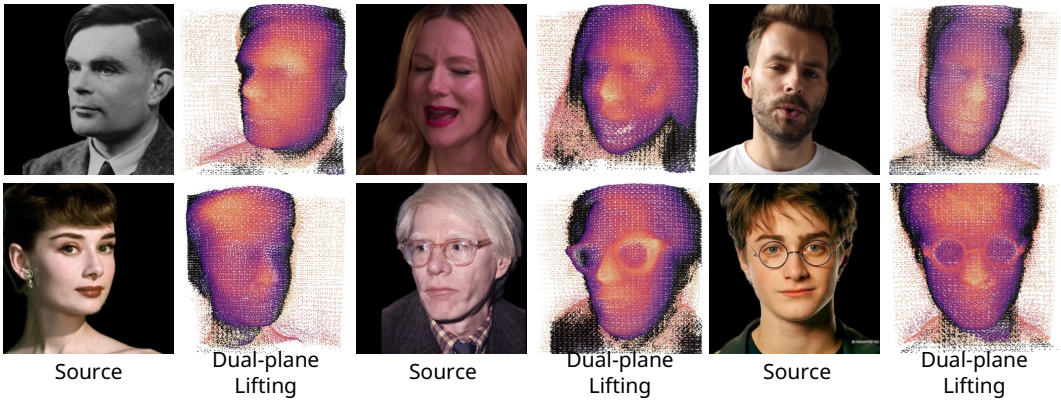

Figure 10: Dual-lifting results of in-the-wild images. We can see that the dual-lifting point cloud has rich details, including glasses and hair. We color the two parts of the dual-lifting separately, and the black points are the image plane.

reconstruct the head's base structure and facial details respectively, which is in line with our expectations. We also show more lifted points in Fig. 10, we can see that the dual-lifting point cloud has rich details, including glasses and hair. Additionally, we provide some lifting point cloud files in supplementary materials.

D More Qualitative Results

We show more self-identity qualitative comparisons with baseline methods in Fig. 11, and cross-identity qualitative comparisons in Fig. 13. Here we show the results of all baseline methods on the VFHQ [Xie et al., 2022] dataset and HDTF [Zhang et al., 2021] dataset.

We also show more results of our method and baseline methods for self and cross-identity reenactment. In Fig. 12, we not only show the reenactment results but also the multi-view results of our method. In Fig. 16, we show more comparisons and consecutive frames and highlight the regions of interest. We also show more in-the-wild results of our method in Fig. 8, 14 and 15. It can be seen that our method maintains good identity consistency and 3D consistency when the viewing angle changes.

Additionally, we provide a supplementary video to demonstrate video driving results. Although no special processing is performed, our method has timing-stable results on video generation.

Figure 11: Self-identity reenactment results on VFHQ [Xie et al., 2022] and HDTF [Zhang et al., 2021] datasets. The top six rows are from VFHQ and the bottom three rows are from HDTF.

Figure 12: Reenactment and multi-view results of our method on the VFHQ [Xie et al., 2022] dataset. Our method can maintain consistency across multiple views.

https://doi.org/10.52202/079017-1838

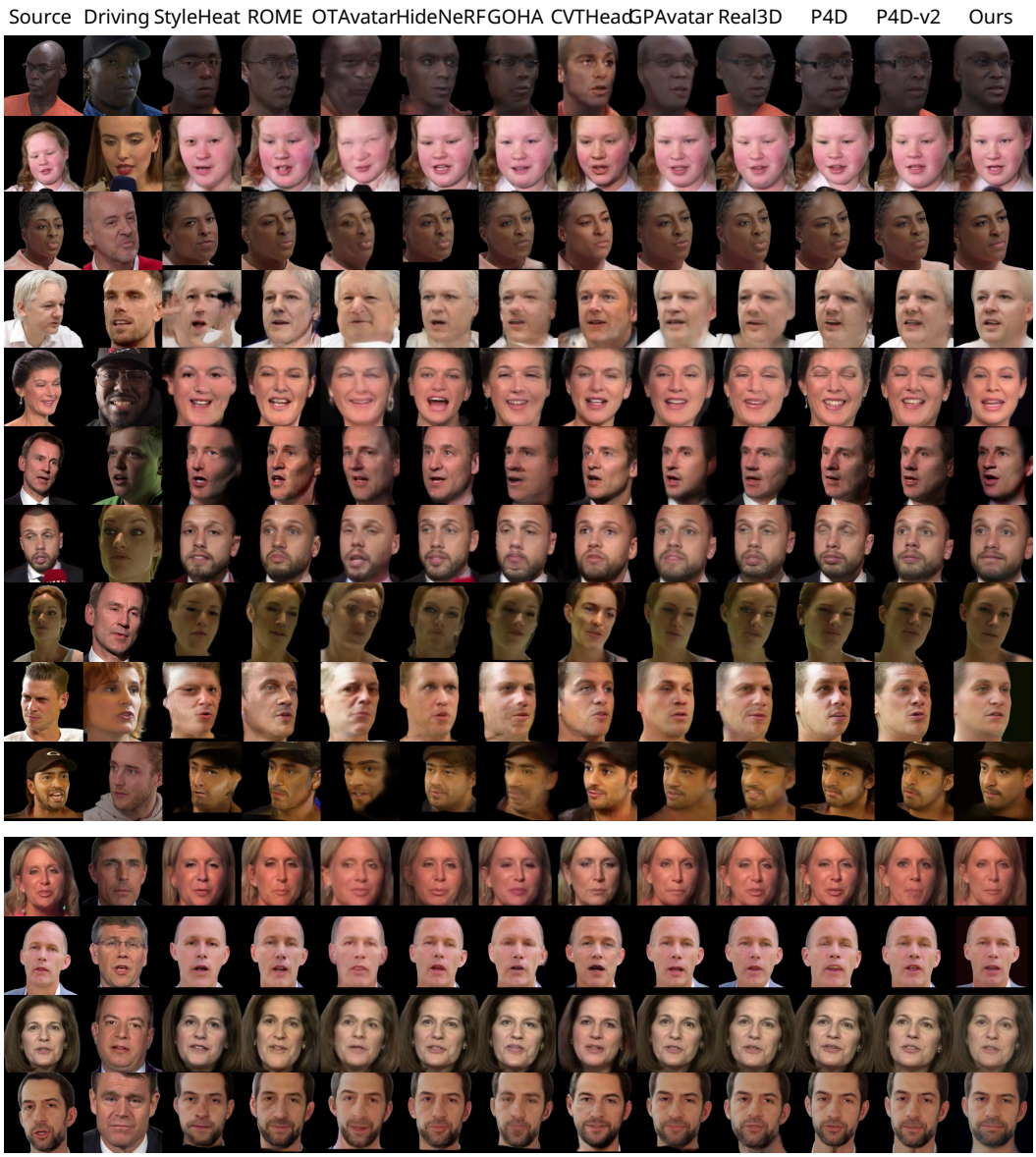

Figure 13: Cross-identity reenactment results on VFHQ [Xie et al., 2022] and HDTF [Zhang et al., 2021] datasets. The top ten rows are from VFHQ and the bottom four rows are from HDTF.

E More In-Depth Ethical Discussion

Our framework offers many applications but also presents ethical risks, such as the potential creation of fake videos ("deepfakes"), violations of privacy, and the dissemination of false information. We do not advocate such misuse and have proposed several measures to prevent these risks:

Watermarking technologies. To ensure transparency and prevent misuse, we plan to employ watermarking techniques in code that will be released. Visible watermarks enable viewers to immediately recognize content as AI-generated, helping them distinguish potential misuse. In addition to visible watermarks, we plan to embed invisible watermarks [Tancik et al., 2020], which are difficult to remove. These invisible marks help track and identify the source of videos, even if they are re-edited. This tracking capability encourages producers to consider the ethical implications and potential risks of their creations by storing information about the video producer.

Strict licenses. We will release our code and model under a strict license. The license will prohibit the synthesis of real individuals without explicit consent for commercial use. This ensures that our

Figure 14: Reenactment and multi-view results of our method on in-the-wild images. From left to right: input image, driving image, driving and novel view results.

https://doi.org/10.52202/079017-1838

Figure 15: Reenactment and multi-view results of our method on in-the-wild images. From left to right: input image, driving image, driving and novel view results.

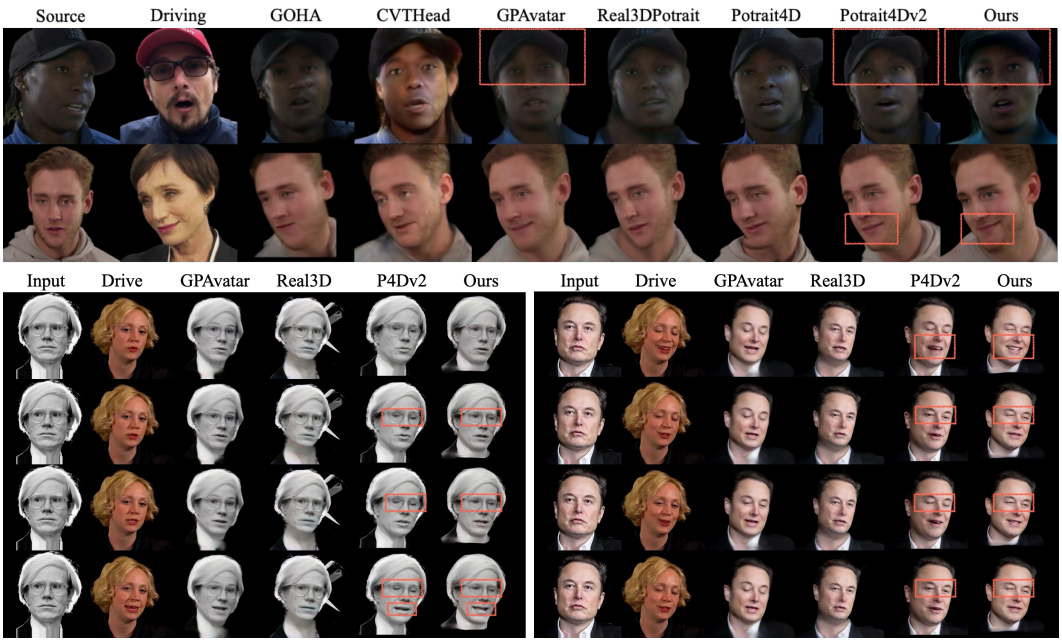

Figure 16: Qualitative results and video continuous frame results with highlighted attention regions. We selected competitive methods to show continuous frames. Better to view it zoomed in.

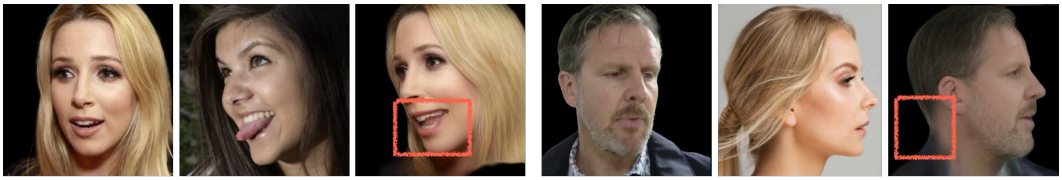

Figure 17: Our model has some limitations. For example, the tongue is not modeled and the unseen regions of the input have less details. Better to view it zoomed in.

technology is used ethically and prevents it from violating the consent of the individual represented by the avatar. Illegal misuse can be traced through the watermark system.

In summary, we will implement robust safeguards to prevent the misuse of our head avatar reconstruction system. We urge video creators to be mindful of the ethical responsibilities and potential risks when using talking face generation technologies. With careful and responsible use, our method can provide substantial benefits across various real-world applications.

F Limitations and Future Work

Although our method achieves high-quality synthesis results compared to previous approaches, there are still some limitations. When rendering synthesized results from novel views, unseen areas in the original source image often lack detail and may produce results with statistically average expectations. For example, generating the other half of the face from a side view input or generating an open mouth from an input image with a closed mouth. Additionally, our expression branch is based on 3DMM and learned from VFHQ video data. This branch may not capture extreme facial movements or parts not modeled by 3DMM, such as one eye being open and the other being closed, the tongue, and hair. We show the qualitative results of these limitations in Fig. 17. Future work may involve learning expression embeddings [Deng et al., 2024b] directly from images, alleviating data requirements and tracking accuracy needs through data generation [Deng et al., 2024a], gathering more expressive data to improve expression imitation. Extending our approach to handle full-body avatar synthesis is also a promising direction for future research.

https://doi.org/10.52202/079017-1838

NeurIPS Paper Checklist

1. **Claims**

   Question: Do the main claims made in the abstract and introduction accurately reflect the paper's contributions and scope?

   Answer: [Yes]

   Justification: The abstract and introduction include the claims made in the paper.

   Guidelines:

   - The answer NA means that the abstract and introduction do not include the claims made in the paper.
   - The abstract and/or introduction should clearly state the claims made, including the contributions made in the paper and important assumptions and limitations. A No or NA answer to this question will not be perceived well by the reviewers.
   - The claims made should match theoretical and experimental results, and reflect how much the results can be expected to generalize to other settings.
   - It is fine to include aspirational goals as motivation as long as it is clear that these goals are not attained by the paper.

2. **Limitations**

   Question: Does the paper discuss the limitations of the work performed by the authors?

   Answer: [Yes]

   Justification: We describe in the limitations and future work section.

   Guidelines:

   - The answer NA means that the paper has no limitation while the answer No means that the paper has limitations, but those are not discussed in the paper.
   - The authors are encouraged to create a separate "Limitations" section in their paper.
   - The paper should point out any strong assumptions and how robust the results are to violations of these assumptions (e.g., independence assumptions, noiseless settings, model well-specification, asymptotic approximations only holding locally). The authors should reflect on how these assumptions might be violated in practice and what the implications would be.
   - The authors should reflect on the scope of the claims made, e.g., if the approach was only tested on a few datasets or with a few runs. In general, empirical results often depend on implicit assumptions, which should be articulated.
   - The authors should reflect on the factors that influence the performance of the approach. For example, a facial recognition algorithm may perform poorly when image resolution is low or images are taken in low lighting. Or a speech-to-text system might not be used reliably to provide closed captions for online lectures because it fails to handle technical jargon.
   - The authors should discuss the computational efficiency of the proposed algorithms and how they scale with dataset size.
   - If applicable, the authors should discuss possible limitations of their approach to address problems of privacy and fairness.
   - While the authors might fear that complete honesty about limitations might be used by reviewers as grounds for rejection, a worse outcome might be that reviewers discover limitations that aren't acknowledged in the paper. The authors should use their best judgment and recognize that individual actions in favor of transparency play an important role in developing norms that preserve the integrity of the community. Reviewers will be specifically instructed to not penalize honesty concerning limitations.

3. **Theory Assumptions and Proofs**

   Question: For each theoretical result, does the paper provide the full set of assumptions and a complete (and correct) proof?

   Answer: [NA]

Justification: The paper does not include theoretical results.

Guidelines:

- The answer NA means that the paper does not include theoretical results.
- All the theorems, formulas, and proofs in the paper should be numbered and cross-referenced.
- All assumptions should be clearly stated or referenced in the statement of any theorems.
- The proofs can either appear in the main paper or the supplemental material, but if they appear in the supplemental material, the authors are encouraged to provide a short proof sketch to provide intuition.
- Inversely, any informal proof provided in the core of the paper should be complemented by formal proofs provided in appendix or supplemental material.
- Theorems and Lemmas that the proof relies upon should be properly referenced.

4. **Experimental Result Reproducibility**

   Question: Does the paper fully disclose all the information needed to reproduce the main experimental results of the paper to the extent that it affects the main claims and/or conclusions of the paper (regardless of whether the code and data are provided or not)?

   Answer: [Yes]

   Justification: We describe in the implementation details section.

   Guidelines:

   - The answer NA means that the paper does not include experiments.
   - If the paper includes experiments, a No answer to this question will not be perceived well by the reviewers: Making the paper reproducible is important, regardless of whether the code and data are provided or not.
   - If the contribution is a dataset and/or model, the authors should describe the steps taken to make their results reproducible or verifiable.
   - Depending on the contribution, reproducibility can be accomplished in various ways. For example, if the contribution is a novel architecture, describing the architecture fully might suffice, or if the contribution is a specific model and empirical evaluation, it may be necessary to either make it possible for others to replicate the model with the same dataset, or provide access to the model. In general. releasing code and data is often one good way to accomplish this, but reproducibility can also be provided via detailed instructions for how to replicate the results, access to a hosted model (e.g., in the case of a large language model), releasing of a model checkpoint, or other means that are appropriate to the research performed.
   - While NeurIPS does not require releasing code, the conference does require all submissions to provide some reasonable avenue for reproducibility, which may depend on the nature of the contribution. For example
     (a) If the contribution is primarily a new algorithm, the paper should make it clear how to reproduce that algorithm.
     (b) If the contribution is primarily a new model architecture, the paper should describe the architecture clearly and fully.
     (c) If the contribution is a new model (e.g., a large language model), then there should either be a way to access this model for reproducing the results or a way to reproduce the model (e.g., with an open-source dataset or instructions for how to construct the dataset).
     (d) We recognize that reproducibility may be tricky in some cases, in which case authors are welcome to describe the particular way they provide for reproducibility. In the case of closed-source models, it may be that access to the model is limited in some way (e.g., to registered users), but it should be possible for other researchers to have some path to reproducing or verifying the results.

5. **Open access to data and code**

   Question: Does the paper provide open access to the data and code, with sufficient instructions to faithfully reproduce the main experimental results, as described in supplemental material?

https://doi.org/10.52202/079017-1838

Answer: [Yes]

Justification: We have included the core code in the supplementary material and will release the full code after refactoring and cleanup. Our data uses publicly available data.

Guidelines:

- The answer NA means that paper does not include experiments requiring code.
- Please see the NeurIPS code and data submission guidelines (https://nips.cc/public/guides/CodeSubmissionPolicy) for more details.
- While we encourage the release of code and data, we understand that this might not be possible, so "No" is an acceptable answer. Papers cannot be rejected simply for not including code, unless this is central to the contribution (e.g., for a new open-source benchmark).
- The instructions should contain the exact command and environment needed to run to reproduce the results. See the NeurIPS code and data submission guidelines (https://nips.cc/public/guides/CodeSubmissionPolicy) for more details.
- The authors should provide instructions on data access and preparation, including how to access the raw data, preprocessed data, intermediate data, and generated data, etc.
- The authors should provide scripts to reproduce all experimental results for the new proposed method and baselines. If only a subset of experiments are reproducible, they should state which ones are omitted from the script and why.
- At submission time, to preserve anonymity, the authors should release anonymized versions (if applicable).
- Providing as much information as possible in supplemental material (appended to the paper) is recommended, but including URLs to data and code is permitted.

6. **Experimental Setting/Details**

   Question: Does the paper specify all the training and test details (e.g., data splits, hyperparameters, how they were chosen, type of optimizer, etc.) necessary to understand the results?

   Answer: [Yes]

   Justification: We describe in the implementation details section.

   Guidelines:

   - The answer NA means that the paper does not include experiments.
   - The experimental setting should be presented in the core of the paper to a level of detail that is necessary to appreciate the results and make sense of them.
   - The full details can be provided either with the code, in appendix, or as supplemental material.

7. **Experiment Statistical Significance**

   Question: Does the paper report error bars suitably and correctly defined or other appropriate information about the statistical significance of the experiments?

   Answer: [No]

   Justification: We use fixed random seeds in all experiments to ensure reproducibility.

   Guidelines:

   - The answer NA means that the paper does not include experiments.
   - The authors should answer "Yes" if the results are accompanied by error bars, confidence intervals, or statistical significance tests, at least for the experiments that support the main claims of the paper.
   - The factors of variability that the error bars are capturing should be clearly stated (for example, train/test split, initialization, random drawing of some parameter, or overall run with given experimental conditions).
   - The method for calculating the error bars should be explained (closed form formula, call to a library function, bootstrap, etc.)
   - The assumptions made should be given (e.g., Normally distributed errors).

- It should be clear whether the error bar is the standard deviation or the standard error of the mean.
- It is OK to report 1-sigma error bars, but one should state it. The authors should preferably report a 2-sigma error bar than state that they have a 96% CI, if the hypothesis of Normality of errors is not verified.
- For asymmetric distributions, the authors should be careful not to show in tables or figures symmetric error bars that would yield results that are out of range (e.g. negative error rates).
- If error bars are reported in tables or plots, The authors should explain in the text how they were calculated and reference the corresponding figures or tables in the text.

8. **Experiments Compute Resources**

   Question: For each experiment, does the paper provide sufficient information on the computer resources (type of compute workers, memory, time of execution) needed to reproduce the experiments?

   Answer: [Yes]

   Justification: We describe in the implementation details section.

   Guidelines:

   - The answer NA means that the paper does not include experiments.
   - The paper should indicate the type of compute workers CPU or GPU, internal cluster, or cloud provider, including relevant memory and storage.
   - The paper should provide the amount of compute required for each of the individual experimental runs as well as estimate the total compute.
   - The paper should disclose whether the full research project required more compute than the experiments reported in the paper (e.g., preliminary or failed experiments that didn't make it into the paper).

9. **Code Of Ethics**

   Question: Does the research conducted in the paper conform, in every respect, with the NeurIPS Code of Ethics https://neurips.cc/public/EthicsGuidelines?

   Answer: [Yes]

   Justification: We fully follow the NeurIPS Code of Ethics.

   Guidelines:

   - The answer NA means that the authors have not reviewed the NeurIPS Code of Ethics.
   - If the authors answer No, they should explain the special circumstances that require a deviation from the Code of Ethics.
   - The authors should make sure to preserve anonymity (e.g., if there is a special consideration due to laws or regulations in their jurisdiction).

10. **Broader Impacts**

    Question: Does the paper discuss both potential positive societal impacts and negative societal impacts of the work performed?

    Answer: [Yes]

    Justification: We discuss it in a broader impacts section.

    Guidelines:

    - The answer NA means that there is no societal impact of the work performed.
    - If the authors answer NA or No, they should explain why their work has no societal impact or why the paper does not address societal impact.
    - Examples of negative societal impacts include potential malicious or unintended uses (e.g., disinformation, generating fake profiles, surveillance), fairness considerations (e.g., deployment of technologies that could make decisions that unfairly impact specific groups), privacy considerations, and security considerations.

https://doi.org/10.52202/079017-1838

- The conference expects that many papers will be foundational research and not tied to particular applications, let alone deployments. However, if there is a direct path to any negative applications, the authors should point it out. For example, it is legitimate to point out that an improvement in the quality of generative models could be used to generate deepfakes for disinformation. On the other hand, it is not needed to point out that a generic algorithm for optimizing neural networks could enable people to train models that generate Deepfakes faster.
- The authors should consider possible harms that could arise when the technology is being used as intended and functioning correctly, harms that could arise when the technology is being used as intended but gives incorrect results, and harms following from (intentional or unintentional) misuse of the technology.
- If there are negative societal impacts, the authors could also discuss possible mitigation strategies (e.g., gated release of models, providing defenses in addition to attacks, mechanisms for monitoring misuse, mechanisms to monitor how a system learns from feedback over time, improving the efficiency and accessibility of ML).

11. **Safeguards**

    Question: Does the paper describe safeguards that have been put in place for responsible release of data or models that have a high risk for misuse (e.g., pretrained language models, image generators, or scraped datasets)?

    Answer: [Yes]

    Justification: We discuss it in the broader impacts section.

    Guidelines:

    - The answer NA means that the paper poses no such risks.
    - Released models that have a high risk for misuse or dual-use should be released with necessary safeguards to allow for controlled use of the model, for example by requiring that users adhere to usage guidelines or restrictions to access the model or implementing safety filters.
    - Datasets that have been scraped from the Internet could pose safety risks. The authors should describe how they avoided releasing unsafe images.
    - We recognize that providing effective safeguards is challenging, and many papers do not require this, but we encourage authors to take this into account and make a best faith effort.

12. **Licenses for existing assets**

    Question: Are the creators or original owners of assets (e.g., code, data, models), used in the paper, properly credited and are the license and terms of use explicitly mentioned and properly respected?

    Answer: [Yes]

    Justification: It is included in the source code.

    Guidelines:

    - The answer NA means that the paper does not use existing assets.
    - The authors should cite the original paper that produced the code package or dataset.
    - The authors should state which version of the asset is used and, if possible, include a URL.
    - The name of the license (e.g., CC-BY 4.0) should be included for each asset.
    - For scraped data from a particular source (e.g., website), the copyright and terms of service of that source should be provided.
    - If assets are released, the license, copyright information, and terms of use in the package should be provided. For popular datasets, `paperswithcode.com/datasets` has curated licenses for some datasets. Their licensing guide can help determine the license of a dataset.
    - For existing datasets that are re-packaged, both the original license and the license of the derived asset (if it has changed) should be provided.

- If this information is not available online, the authors are encouraged to reach out to the asset's creators.

13. **New Assets**

    Question: Are new assets introduced in the paper well documented and is the documentation provided alongside the assets?

    Answer: [No]

    Justification: We are not ready to release our model yet.

    Guidelines:

    - The answer NA means that the paper does not release new assets.
    - Researchers should communicate the details of the dataset/code/model as part of their submissions via structured templates. This includes details about training, license, limitations, etc.
    - The paper should discuss whether and how consent was obtained from people whose asset is used.
    - At submission time, remember to anonymize your assets (if applicable). You can either create an anonymized URL or include an anonymized zip file.

14. **Crowdsourcing and Research with Human Subjects**

    Question: For crowdsourcing experiments and research with human subjects, does the paper include the full text of instructions given to participants and screenshots, if applicable, as well as details about compensation (if any)?

    Answer: [NA]

    Justification: The paper does not involve crowdsourcing nor research with human subjects.

    Guidelines:

    - The answer NA means that the paper does not involve crowdsourcing nor research with human subjects.
    - Including this information in the supplemental material is fine, but if the main contribution of the paper involves human subjects, then as much detail as possible should be included in the main paper.
    - According to the NeurIPS Code of Ethics, workers involved in data collection, curation, or other labor should be paid at least the minimum wage in the country of the data collector.

15. **Institutional Review Board (IRB) Approvals or Equivalent for Research with Human Subjects**

    Question: Does the paper describe potential risks incurred by study participants, whether such risks were disclosed to the subjects, and whether Institutional Review Board (IRB) approvals (or an equivalent approval/review based on the requirements of your country or institution) were obtained?

    Answer: [NA]

    Justification: The paper does not involve crowdsourcing nor research with human subjects.

    Guidelines:

    - The answer NA means that the paper does not involve crowdsourcing nor research with human subjects.
    - Depending on the country in which research is conducted, IRB approval (or equivalent) may be required for any human subjects research. If you obtained IRB approval, you should clearly state this in the paper.
    - We recognize that the procedures for this may vary significantly between institutions and locations, and we expect authors to adhere to the NeurIPS Code of Ethics and the guidelines for their institution.
    - For initial submissions, do not include any information that would break anonymity (if applicable), such as the institution conducting the review.

https://doi.org/10.52202/079017-1838